Research Article

Effects of CeO_2 on the microstructure and properties of 2A12 porous aluminum

Chao Liu[1,2] · Yang Liu[1,2] · Yunzhu Ma[1,2] · Wensheng Liu[1,2] · Yuling Yang[1,2]

Abstract
The micron porous aluminum has received considerable attention in various domains, and the research of rare earths for the synthesis of materials with improved mechanical performance. In the present work, 2A12 aluminum alloys with different porosities were successfully prepared by cold pressing-vacuum sintering-dissolution process (SDP) with the CeO_2 additive, and the CeO_2 content effect on the microstructure and mechanical properties of the porous aluminum alloys were investigated. The results show that the open-cell porous aluminum with uniform holes can be obtained by SDP. CeO_2 addition affects the microstructure of porous aluminum alloys and results in the formation of $Al_{11}Ce_3$ phase in specimens, which can enhance mechanical properties of the alloys. With increasing content of CeO_2, all the specimens have a trend of increasing first and then decreasing, and when the CeO_2 content equal to 0.2 wt%, the tensile and compression strengths of porous aluminum with different porosities achieved the maximum value.

Keywords 2A12 porous aluminum · CeO_2 · Microstructure · $Al_{11}Ce_3$ · Tensile and compression strengths

1 Introduction

Cellular metallic materials have attracted attention in the last decades with the availability of practical manufacturing technologies and improved understanding of their physical, chemical and mechanical properties. Aluminum is one of the very few metals with applications from utensils to aircraft parts. Although aluminum surface is protected by the oxide layer, this layer can still be damaged in aggressive environments leading to fast corrosion. Different additives can be introduced into the aluminum matrix to improve its microstructure and other properties [1, 2].

Porous aluminum alloy is a very popular advanced composite material because of its attractive physical and mechanical properties, such as light weight, high strength, good energy absorption, excellent shock resistance, damp shock absorption, etc. Based on the connectivity of cells, cellular metals can be categorized as either closed- or open-celled. Cellular metals are also dominantly used for construction, auto parts, electronic equipment, aerospace, and other broad variety of fields [3–7].

Rare earths (RE) elements incorporated into the aluminum structure inhibit its recrystallization, grain refinement and influence the precipitation process. RE elements additions also improve mechanical and physical properties of aluminum as a conductor [8–12]. Additions of such RE elements as Er, Sc, Ce and La were studied with regard of their beneficial effects on the mechanical properties of aluminum alloys. The most benefits were obtained at low RE elements concentrations [13–20].

However, the effects of CeO_2 addition on the microstructure and mechanical properties of the porous aluminum alloys obtained by powder metallurgy have not been investigated systematically. In this study, we used

✉ Yunzhu Ma, zhuzipm@csu.edu.cn; ✉ Wensheng Liu, liuwensheng@csu.edu.cn; Chao Liu, mseliuchao@csu.edu.cn; Yang Liu, liuyang7740038@163.com; Yuling Yang, 631695016@qq.com | [1]State Key Laboratory of Powder Metallurgy, Central South University, Changsha 410083, People's Republic of China. [2]State Key Laboratory of Lightweight and High Strength Structural Materials, Central South University, Changsha 410083, People's Republic of China.

SN Applied Sciences (2019) 1:111 | https://doi.org/10.1007/s42452-018-0127-3

Received: 12 August 2018 / Accepted: 12 December 2018 / Published online: 18 December 2018

Table 1 Chemical composition of the 2A12 aluminum powder, wt%

Cu	Mg	Mn	Fe	Si	Cr	Zn	Ti	Al
4.09	1.18	0.54	0.21	0.12	0.10	0.06	0.02	Balance

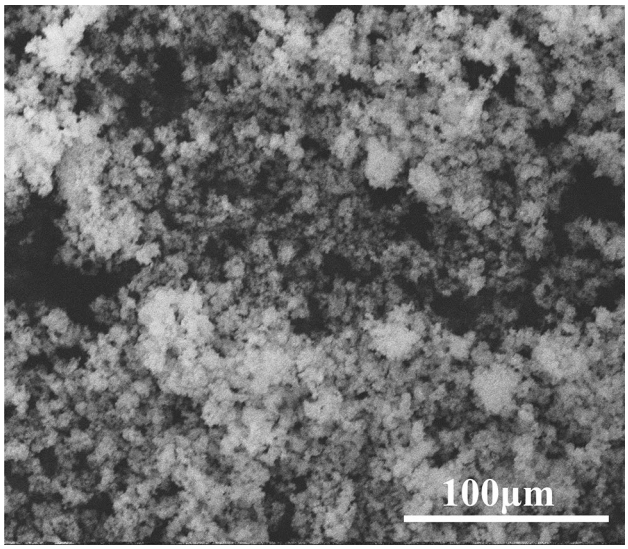

Fig. 1 Microstructure of the CeO_2 powder

Table 2 Nominal composition of specimen powders (mass fraction %)

Academic porosity (%)	Sample number	RE
Group A-30%	Alloy 1	0
	Alloy 2	0.2
	Alloy 3	0.4
	Alloy 4	0.6
	Alloy 5	0.8
	Alloy 6	1.0
Group B-50%	Alloy 1	0
	Alloy 2	0.2
	Alloy 3	0.4
	Alloy 4	0.6
	Alloy 5	0.8
	Alloy 6	1.0

SDP technique to prepare 2A12 porous aluminum alloys with different porosity. We studied the influence of CeO_2 addition on phase evolution, microstructure and mechanical properties of porous Al alloys at room temperature.

2 Materials and methods

The initial materials were 2A12 aluminum alloy powder (see Table 1 for its chemical composition) with 99.9% purity and 8–15 μm particle sizes, hydrosoluble filler with 99.9% purity and 40–55 μm particle diameters and CeO_2 powder with 99.99% purity and 10–15 nm diameters. The microstructure of CeO_2 powder is shown in Fig. 1.

The porous aluminum alloys with 30 (group A) and 50% (group B) porosity were prepared by SDP. CeO_2 content for different samples is shown in Table 2. The composite powders were prepared by V-blender mixer for 3 h at the milling speed of 30 r/min. The two action pressures were adopted to make green compacts at 200 MPa. The samples had the dimension of Φ40 × 5 mm. Wu et al. [21] measure the liquid volume fraction and his results indicated that the actual freezing range of 2A12 aluminum alloy powder is 509–648.3 °C. Thus, we sintered the green compacts in vacuum at 650 °C for 270 min. The sintering was performed using melted samples the liquid metal viscosity is sufficient penetrate between WSG particles. After sintering, the alloys were cooled to the room temperature at 10 °C/min. The pore former of the sintered samples was dissolved in water at a temperature of 60 °C.

The X-ray diffraction (XRD) analysis was performed at room temperature using D/MAX-2550X diffractometer with Cu-K_α radiation. The surface and fracture microstructure of polished samples were studied using scanning electron microscopy (SEM, FEI Nano230) equipped with energy dispersive spectroscopy (EDS). The chemical analysis was performed by electron probe micro-analysis (EPMA) using a JXA-8530F. The tensile and compression strengths were tested with an INSTRON 3369 with the loading speed of 0.5 mm/min.

3 Results and discussion

3.1 XRD analysis

XRD patterns of all samples in the group A are shown in Fig. 2 in comparison with the CeO_2-free alloy #1. Four phases were detected at low CeO_2 content: metallic Al, Al_2O_3, AlCuMg and $MgAl_2O_4$. As the CeO_2 content increases, new phase $Al_{11}Ce_3$ appears in the XRD patterns. Incorporation of the CeO_2 in the aluminum matrix is not evident because of the very negligible XRD peak shifts.

The following reactions may occur when the CeO_2 was added to 2A12 aluminum [22]:

$$3/2CeO_2 + 2Al \rightarrow Al_2O_3 + 3/2Ce + \Delta H_1, \quad (1)$$

$$11Al + 3Ce \rightarrow Al_{11}Ce_3 + \Delta H_2. \quad (2)$$

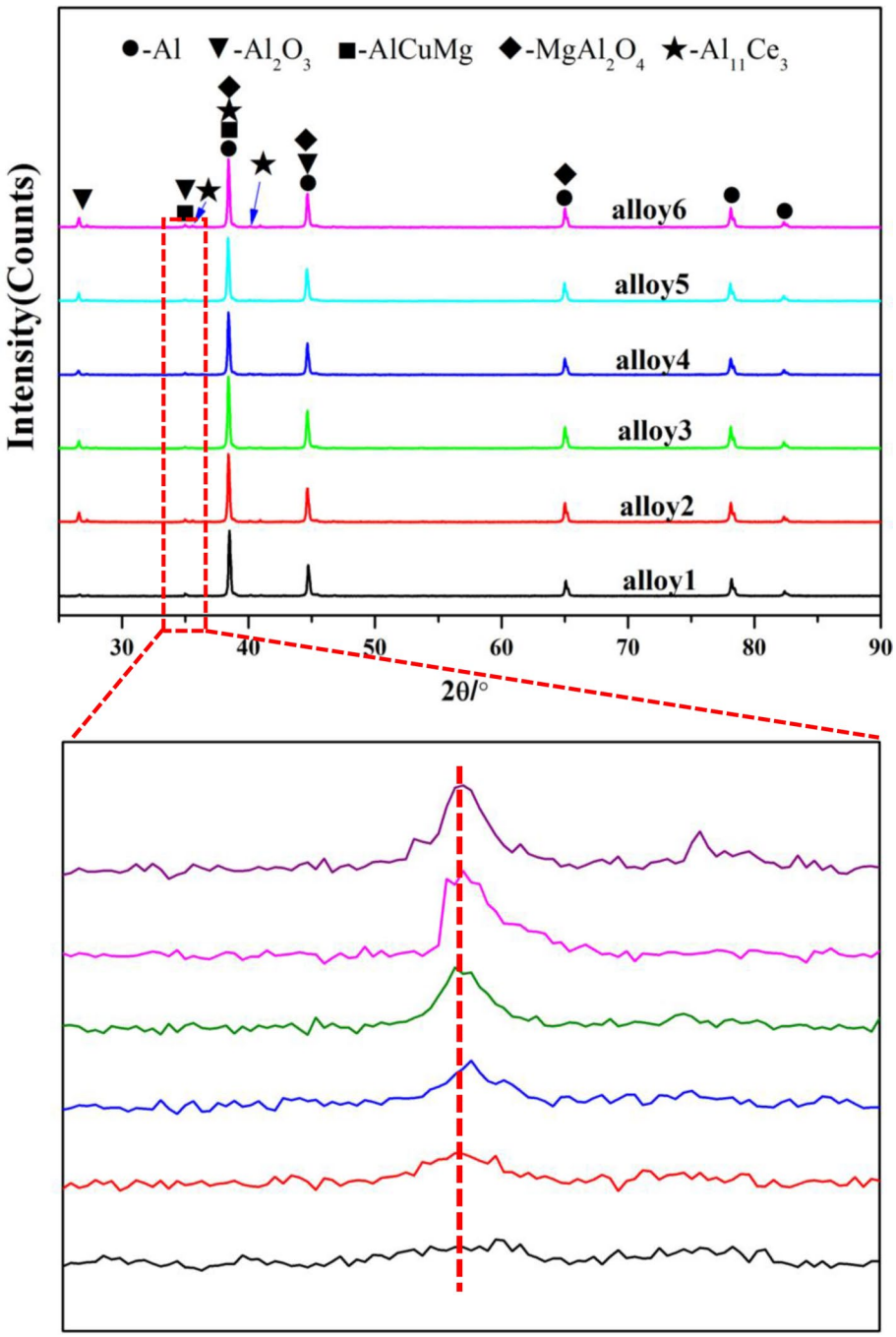

Fig. 2 The XRD patterns of the alloys from the A-group with different CeO_2 content

Both reaction (1) and (2) are exothermic with $\Delta H_1 = -44.1$ kJ/mol and $\Delta H_2 = -574$ kJ/mol. The Al–$Al_{11}Ce_3$ eutectic is formed in the Al–rich side of the Al–Ce binary phase diagram at 913 K. The heat released from the Al–CeO_2 reaction may cause the eutectic melting of Al and $Al_{11}Ce_3$. Because of that the heat is rapidly lost to the surrounding aluminum matrix, and the melting only occurs locally and resolidification follows. It is suggested that the microstructure consisting of round Al–rich phase enclosed by $Al_{11}Ce_3$ may result from the local melting and resolidification of material with a hypereutectic Al–$Al_{11}Ce_3$ composition. From the thermodynamic point of view, the addition of CeO_2 may reduce the sintering temperature of 2A12 alloy and promote the sintering process.

3.2 Microstructure analysis

Figure 3 shows the SEM images of 2A12 aluminum with different porosity and CeO_2 amounts. Less white phase is observed (see Fig. 3a) as the CeO_2 amount changed,

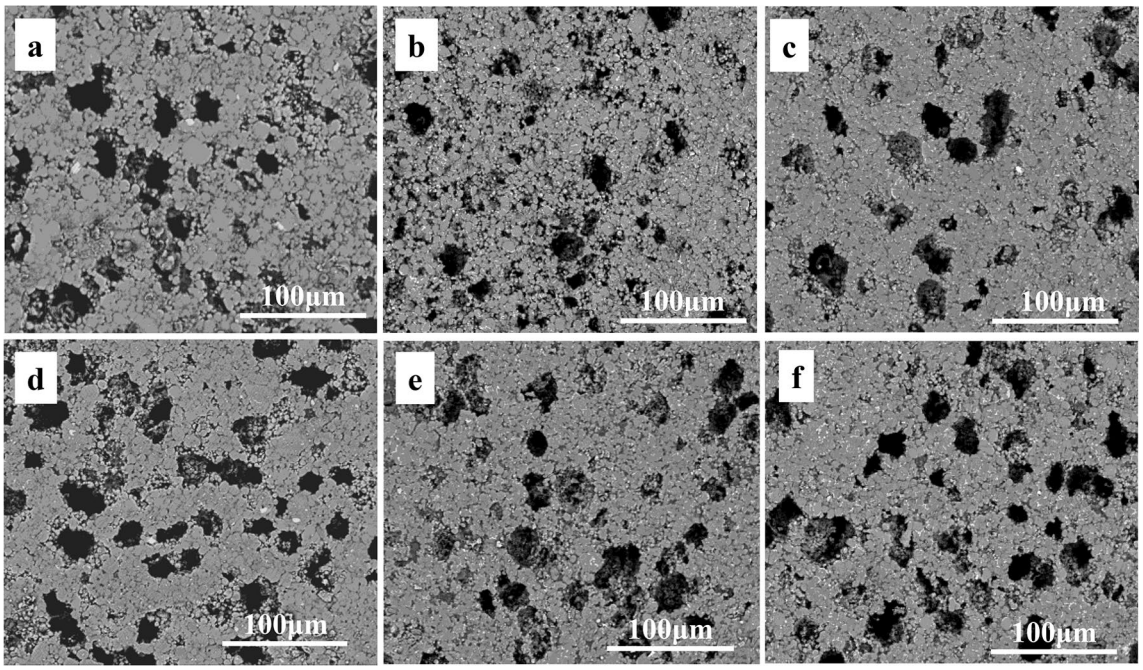

Fig. 3 SEM micrographs of porous aluminum with different CeO_2 content. **a** A + alloy 1, **b** A + alloy 3, **c** A + alloy 6, **d** B + alloy 1, **e** B + alloy 3, **f** B + alloy 6

implying that the aluminum alloy achieved a good compactness. The microstructures of samples in the Group A can be described by two different colored areas. The content of white precipitated phase increased (see Fig. 3a–c): CeO_2 addition reduced grain size of aluminum powder and increased the white precipitated phase content (see Fig. 3d–f). However, it is not obvious that the CeO_2 has grain refining effect on the casting aluminum alloy. The pore distribution of porous aluminum is uniform, and it has open-pore structure, which can effectively dissolve the pore-forming agent. The samples showed no obvious collapse after sintering, and the pores were uniformly distributed and had diameters ~ 80 μm. The white precipitated phases have granular or rod-like shape and are mainly observed at the granule boundaries.

The results of EDS are show in Fig. 4, and the gray part can be described as Al–Cu–Mg intermediate phase while the white part can be a mixture of Al–Cu–Mg and $Al_{11}Ce_3$ phases. These results agree with the XRD results. Solubility of RE elements in aluminum matrix is very small [22–24] and typically RE elements cannot be detected by just EDS.

Results of EPMA analysis of the alloys from group A are shown in Fig. 5. Distribution of Al, Cu, Mg, O and Ce is shown by the color ranging from blue to red. Aluminum (see Fig. 5b) is found in all parts of the sample with the exception of the pores. Aluminum content is small in the dark grey area (see Fig. 5a). Spectral analysis shown in Fig. 5c showed that the dark grey area scorrespond to the oxidized aluminum judging by the distribution of O shown in Fig. 5e. Distribution of Cu, Mg and Ce is almost identical to the position of white precipitated phase in Fig. 5a. These white phases are located between aluminum granules. According to the analysis described above, the white precipitated phase consists of Al–Cu–Mg intermediate phase and $Al_{11}Ce_3$.

3.3 Mechanical properties analysis

The tensile and compression strengths of sintered samples with different porosity and CeO_2 additions were measured at room temperature (see Fig. 6), and the strain rates are 0.001/s and 0.0015/s, respectively. Both tensile and compression strengths for both groups A and B first increased but then decreased with the increasing CeO_2 content (see Fig. 6a). The tensile and compression strengths of aluminum with 30% porosity are 32.8 and 70.6 MPa, respectively. The maximum values of tensile and compression strengths were 48.1 and 77.8 MPa, respectively, at CeO_2 content equal to 0.2 wt%. CeO_2 content increase from 0 to 0.2 wt% resulted in the fastest tensile and compressive strengths increase: 48.2% and 11.2%, respectively. Group B samples with 50% porosity showed similar results (see Fig. 6b). The best tensile and compression strengths were obtained again at 0.2 wt% of CeO_2 and are equal to 24.9 and 32.6 MPa, respectively.

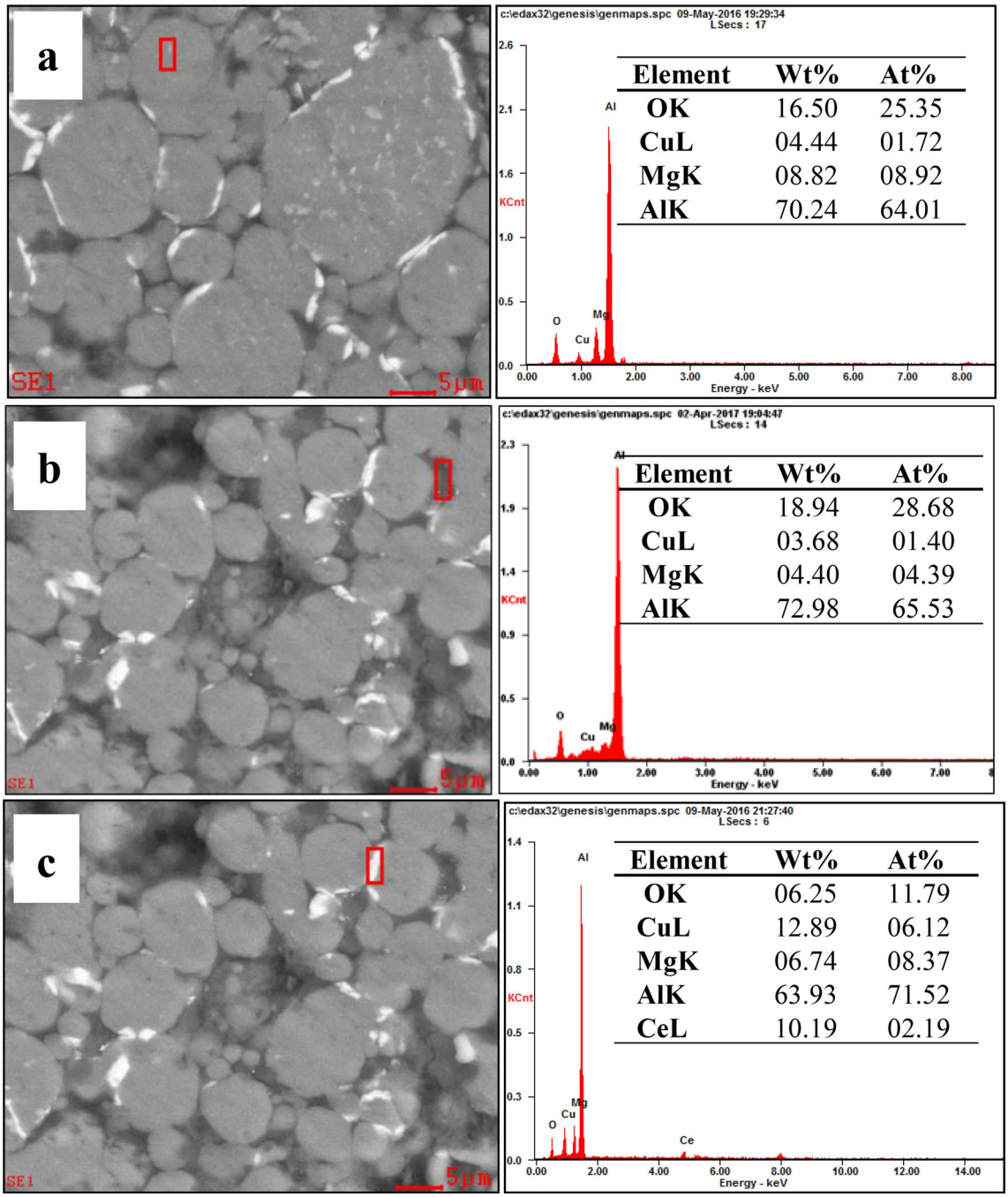

Fig. 4 EDS analysis of selected areas of the alloy 6 from the group A

Under the same conditions, the compressive strength of porous aluminum is much higher than its tensile strength, which is related to the structural characteristics of porous aluminum. Because of the pores presence, the tensile strength of the porous aluminum is sensitive to the crack due to the stress concentration, while the compression strength is not affected by this. In addition, the content of CeO_2 has no influence on the pore size and morphology of 2A12 alloys. Since certain conditions are required for particles to grow during the sintering process, we believe that alloys can achieve better properties with the CeO_2 addition.

Ce can either form solid solution with aluminum and its alloys, or accumulate in the interface between grain and phase boundaries, or form an intermetallic compounds with aluminum. The metallic Ce and Al have h.c.p. and f.c.c. crystal structures, respectively. Addition of Ce into the Al structure can form limited solid solution [25]. However, Ce

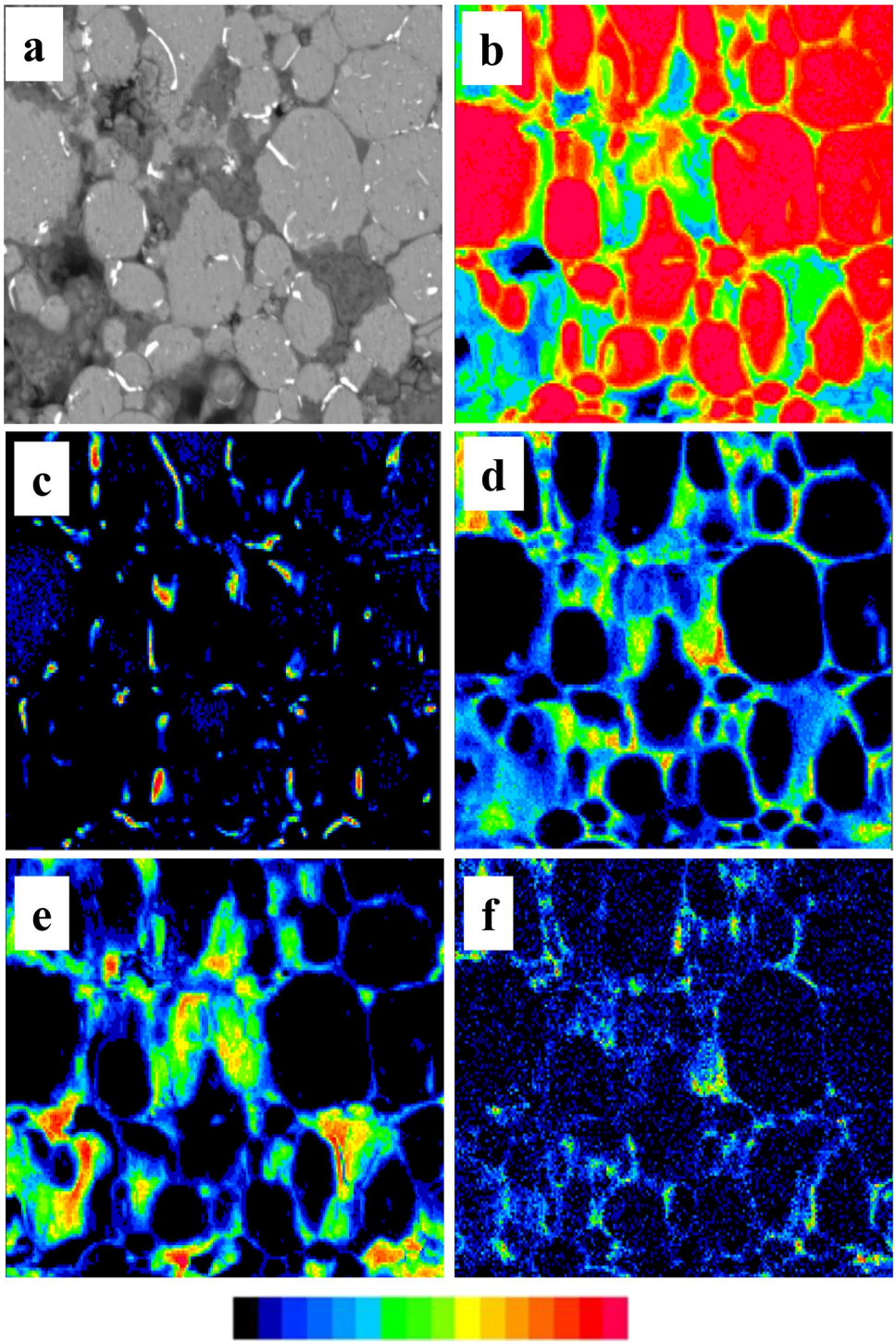

Fig. 5 The elements distribution of A + alloy 6. **a** selected area, **b** Al, **c** Cu, **d** Mg, **e** O, **f** Ce

can accumulate at the interface with the aluminum alloy to form the intermetallic compound. This can affect the distribution of precipitated phases and the deformation resistance of aluminum alloys, both of which are beneficial to the mechanical properties enhancement.

The improvement of mechanical properties of sintered samples can be explained by the fracture mechanism. SEM images of fracture microstructure are shown in Fig. 7. However, the number and depth of toughness nest increased with increase the CeO_2 content, and the intergranular and transgranular fractures coexisted in the alloy. The EDS analysis of toughness nest of the sintered alloys with CeO_2 is shown in Fig. 7d. The fracture area of the sample corresponds to the area of the precipitated phase, thus, we believe that CeO_2 addition can effectively promote Al–Cu–Mg phase separation from the $Al_{11}Ce_3$

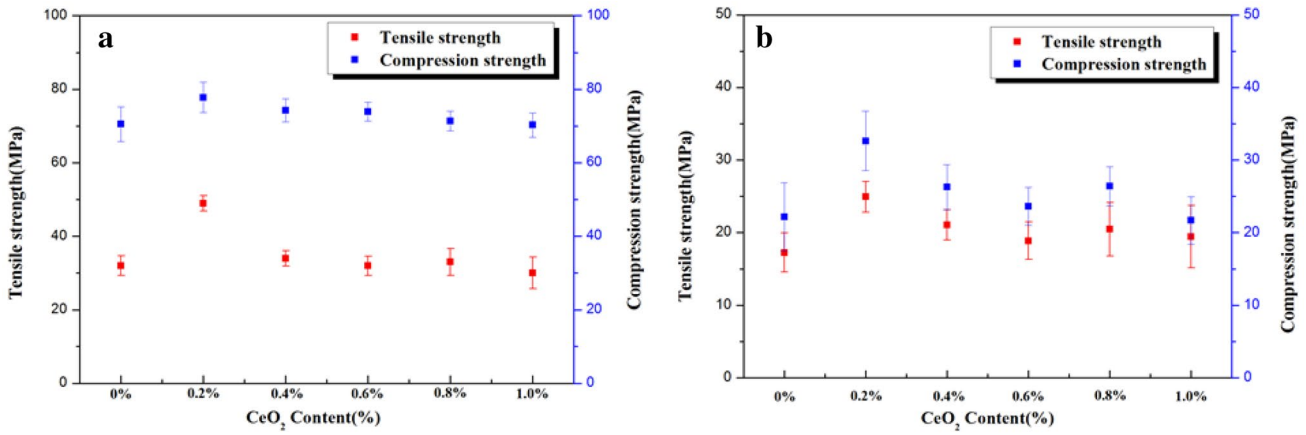

Fig. 6 The tensile and compression strengths of sintered samples with different porosity and CeO_2 additions, **a** 30% porosity, **b** 50% porosity

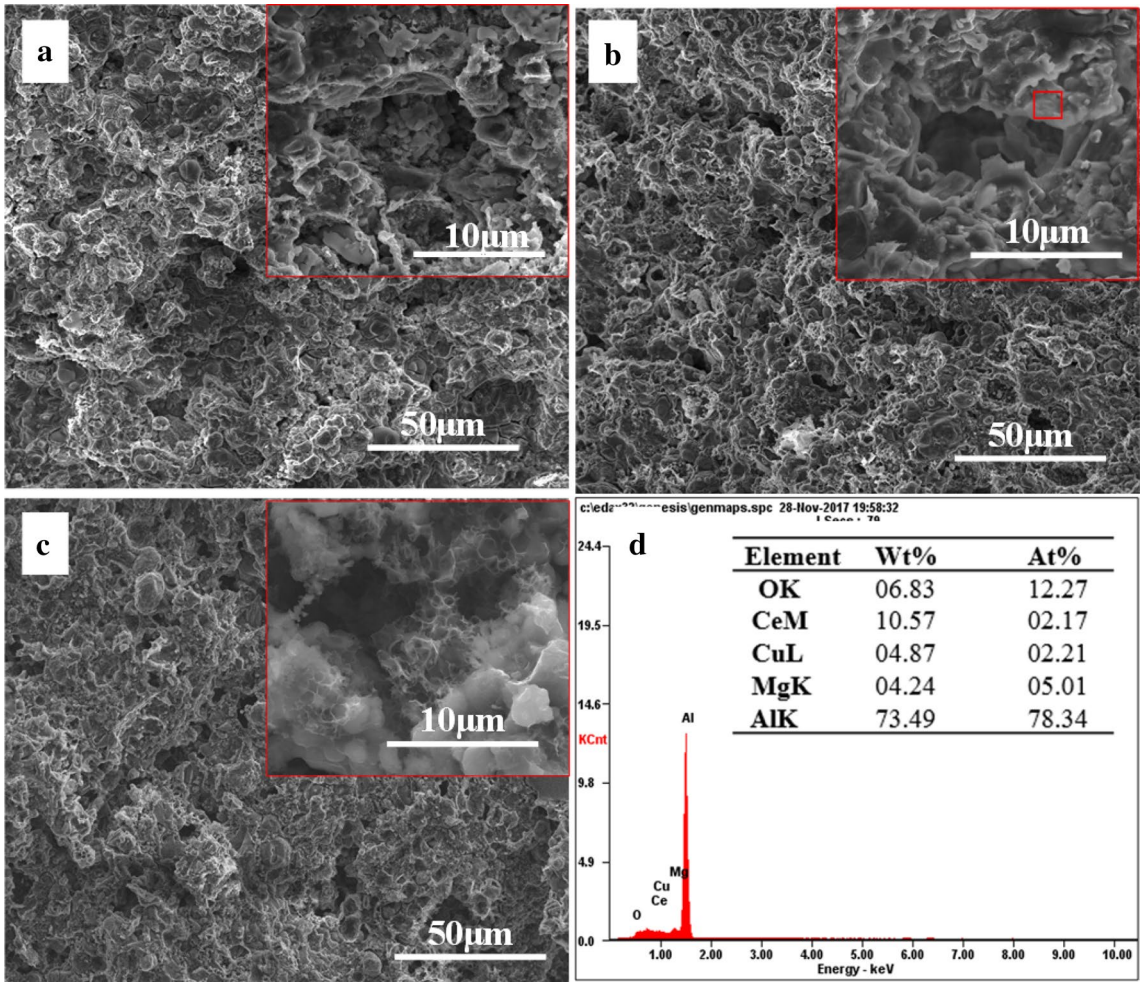

Fig. 7 The fracture micrographs of porous aluminum with different CeO_2 contents. **a** A + alloy 1, **b** A + alloy 2, **c** A + alloy 6, **d** EDS of red area in **b**

phase. The $Al_{11}Ce_3$ phase causes the lattice distortion in the aluminum matrix with high distortion energy. This phase can strengthen both the grain and phase boundaries. However, the stress concentration appeared at very high $Al_{11}Ce_3$ content diminishing the performance of the sintered alloys. Thus, only the certain amount of CeO_2 can improve the mechanical properties of 2A12 porous aluminum alloys [26–28].

4 Conclusions

The micron porous aluminum alloys with different porosities were successfully prepared by the cold pressing-vacuum sintering-dissolution. The CeO_2 changed the microstructure of porous aluminum alloys and resulted in the formation of $Al_{11}Ce_3$ phase, which enhanced the mechanical properties of the hosting matrix. When the CeO_2 addition was 0.2 wt%, the tensile and compression strengths of porous aluminum achieved the maximum values.

Acknowledgements This study was funded by the National Basic Research Program of China (Grant No. 61xxxx02).

Compliance with ethical standards

Conflict of interest The authors declared that they have no conflict of interest.

References

1. Kamaraj K, Devarapalli R, Siva T, Sathiyanarayanan S (2015) Self-healing electrosynthesied polyaniline film as primer coat for AA2024-T3. Mater Chem Phys 153:256–265
2. Saeedikhani M, Javidi M, Vafakhah S (2017) Anodising of 2024-T3 aluminum alloy in electrolyte of sulphuric–boric–phosphoric mixed acid containing cerium salt as corrosion inhibitor. Trans Nonferr Met Soc China 27:711–721
3. Mu Y, Yao G, Luo H (2010) Effect of cell shape anisotropy on the compressive behavior of closed-cell aluminum foams. Mater Des 31:1567–1569
4. Zhang LC, He AQ, Ye HQ, Huang C, Zhang YC (2002) Characterization of dispersed intermetallic phases in an Al–8.32 wt%Fe–3.4 wt%Ce alloy. J Mater Sci 37:5183–5189
5. Baoyo JM (2017) Open-cell porous metals for thermal management applications. Fluid flow and heat transfer. Mater Sci Technol 33:265–276
6. Mukherjee M, García-Moreno F, Jiménez C, Rack A, Banhartbd J (2017) Microporosity in aluminum foams. Acta Mater 131:156–168
7. An YK, Yang SY, Wu HY, Zhao ET, Wang ZS (2017) Investigating the internal structure and mechanical properties of graphene nanoflakes enhanced aluminum foam. Mater Des 134:44–53
8. Wang WT, Zhang XM, Gao ZG, Jia YZ, Ye LY, Zheng DW, Liu L (2010) Influences of Ce addition on the microstructures and mechanical properties of 2519A aluminum alloy plate. J Alloys Compd 491:366–371
9. Chen KH, Fang HC, Zhang Z, Chen X, Liu G (2008) Effect of of Yb, Cr and Zr additions on recrystallization and corrosion resistance of Al–Zn–Mg–Cu alloys. Mater Sci Eng A 497:426–431
10. Gordillo MA, Cernatescu I, Aindow TT, Watson TJ, Aindow M (2014) Phase stability in a powder-processed Al–Mn–Ce alloy. J Mater Sci 49:3742–3754
11. Xiao DH, Huang BY (2007) Effect of Yb addition on precipitation and microstructure of Al–Cu–Mg–Ag alloys. Trans Nonferr Met Soc China 17:1181–1185
12. Li HZ, Ling XP, Li FF, Guo FF, Li Z, Zhang XM (2007) Effect of Y content on microstructure and mechanical properties of 2519 aluminum alloy. Trans Nonferr Met Soc China 17:1194–1198
13. Prukkanon W, Srisukhumbowornchai N, Limmaneevichitr C (2009) Influence of Sc modification on the fluidity of an A356 aluminum alloy. J Alloys Compd 487(1–2):453–457
14. Zhang JH, Yu P, Liu K, Fang DQ, Tang DX, Meng J (2009) Effect of substituting cerium-rich mischmetal with lanthanum on microstructure and mechanical properties of diecast Mg–Al–RE alloys. Mater Des 30(7):2372–2378
15. Li PF, Wu ZG, Wang YL, Gao XZ, Wang ZY, Li ZQ (2006) Effect of cerium on mechanical performance and electrical conductivity of aluminum rod for electrical purpose. J Rare Earth 24:355–357
16. Govindaraju HK, Jayaraj T, Sadanandarao PR, Venkatesha CS (2010) Evaluation of mechanical properties of as-cast Al–Zn–Ce alloy. Mater Des 31:S24–S29
17. Chen ZW, Chen P, Li SS (2012) Effect of Ce addition on microstructure of $Al_{20}Cu_2Mn_3$ twin phase in an Al–Cu–Mn casting alloy. Mater Sci Eng A 532:606–609
18. Kiyota S, Valdez B, Stoytcheva M, Zlatev R, Bastidas JM (2011) Anticorrosion behavior of conversion coatings obtained from unbuffered cerium salts solutions on AA6061-T6. J Rare Earth 29:961–968
19. Zhang GJ, Liu G, Sun YJ, Jiang F, Wang L, Wang RH, Sun J (2009) Microstructure and strengthening mechanisms of molybdenum alloy wires doped with lanthanum oxide particles. Int J Refract Met Hard Mater 27(1):173–176
20. Tsai YC, Chou CY, Lee SL, Lin CK, Lin JC, Lim SW (2009) Effect of trace La addition on the microstructures and mechanical properties of A356 (Al–7Si–0.35Mg) aluminum alloys. J Alloys Compd 487:157–162
21. Wu M, Liu YZ, Wang T, Yu KB (2016) Deformation behavior and characteristics of sintered porous 2024 aluminum alloy compressed in a semisolid state. Mater Sci Eng A 674:144–150
22. Chen CF, Kao PW, Chang LW (2010) Effect of processing parameters on microstructure and mechanical properties of an Al–$Al_{11}Ce_3$–Al_2O_3 in situ composite produced by friction stir processing. Metall Mater Trans A 41:513–522
23. Yin FC, Su XP, Li Z, Shi Y, Zhang P (2000) A thermodynamic assessment of Ce–Al system. Rare Met 19:255–260
24. Cao ZJ, Kong G, Che CS, Wang YQ, Peng HT (2017) Experimental investigation of eutectic point in Al–rich Al–La, Al–Ce, Al–Pr and Al–Nd systems. J Rare Earth 35:1022–1028
25. Du WW, Sun YS, Min XG (2003) Microstructure and mechanical properties of Mg–Al based alloy with calcium and rare earth additions. Mater Sci Eng A 356:1–7
26. Yang CC, Hsu WM, Chang E (2013) Wear performance of Al–Fe–V–Si particle reinforced cast aluminum alloy composites. Mater Sci Technol 13:687–694
27. Xiao DH, Wang JN, Ding DY (2003) Effect of rare earth Ce addition on the microstructure and mechanical properties of an Al–Cu–Mg–Ag alloy. J Alloys Compd 352:84–88
28. Zhou J, Gao Z, Cuitino AM (2004) Effects of heat treatment on the compressive deformation behavior of open cell aluminum foams. Mater Sci Eng A 386:118–128